Acta Cryst C STRUCTURAL CHEMISTRY

ISSN 2053-2296

Nucleophilic substitution of a phthalimidyl group with morpholine in an N^1-methyl-1,2,3-triazole: crystallographic evidence for migration of the methylene bridge

Paul R. Palme,[a] Richard Goddard,[b] Markus Leutzsch,[b] Adrian Richter,[a] Peter Imming[a] and Rüdiger W. Seidel[a]*

[a]Institut für Pharmazie, Martin-Luther-Universität Halle-Wittenberg, Wolfgang-Langenbeck-Strasse 4, 06120 Halle (Saale), Germany, and [b]Max-Planck-Institut für Kohlenforschung, Kaiser-Wilhelm-Platz 1, 45470 Mülheim an der Ruhr, Germany. *Correspondence e-mail: ruediger.seidel@pharmazie.uni-halle.de

Received 28 January 2026
Accepted 16 March 2026

Edited by M. Yousufuddin, University of North Texas at Dallas, USA

This article is part of the collection *Early Career Scientists in Structural Science* and is dedicated to Dr Dietrich Seidel on the occasion of his 70th birthday.

Keywords: 1,2,3-triazole; click chemistry; 1,3-dipolar cycloaddition; substituent migration; Hirshfeld atom refinement; crystal structure.

CCDC references: 2538228; 2538227

Supporting information: this article has supporting information at journals.iucr.org/c

2-{[4-(4-Bromophenyl)-1*H*-1,2,3-triazol-1-yl]methyl}phthalimide, $C_{17}H_{11}BrN_4O$, was synthesized by click chemistry employing a copper-catalyzed azide–alkyne 1,3-dipolar cycloaddition. The molecule adopts an angular structure and was found to crystallize in the monoclinic system (space group $P2_1/n$, $Z = 4$). Reaction with morpholine in the presence of a base afforded 4-{[4-(4-bromophenyl)-2*H*-1,2,3-triazol-2-yl]methyl}morpholine, $C_{13}H_{15}BrN_4O$, as the major product, involving a nucleophilic substitution of morpholine for the phthalimide group and migration of the substituent from N1 to N2 on the 1,2,3-triazole ring. The morpholine-substituted compound likewise crystallizes in the monoclinic system (space group $P2_1/c$, $Z = 4$) with the molecule exhibiting an angular shape. Both crystal structures appear to be governed by close packing, with weak C—H···O and C—H···N hydrogen bonds as the prevailing intermolecular interactions.

1. Introduction

1,2,3-Triazoles are aromatic heterocyclic compounds featuring a five-membered ring with three adjacent N atoms, characterized by their 1*H*- and 2*H*-tautomeric forms (Moura & Tomé, 2022). The 1,2,3-triazole system has gained much importance in the fields of organic chemistry (Haldón *et al.*, 2015; Dai *et al.*, 2022; Vala *et al.*, 2022), agriculture (Song *et al.*, 2024), materials science (Verma *et al.*, 2026) and medicinal chemistry (Bonandi *et al.*, 2017; Bozorov *et al.*, 2019; Marzi *et al.*, 2022; Farwa *et al.*, 2025). Several 1,2,3-triazole-containing drugs, for example, the cephalosporin antibiotic cefatrizine, the β-lactamase inhibitor tazobactam, the oxazolidone antibiotic radezolid, the anticonvulsant rufinamide and the orexin receptor antagonist suvorexant, are on the market.

In medicinal chemistry, interest in the 1,2,3-triazole heterocycle can be largely attributed to its capability to serve as a bioisostere for several functional groups (Bonandi *et al.*, 2017) and as a linking group in 1,2,3-triazole-containing hybrids. In the latter field, significant progress has been achieved through the development of copper-catalyzed azide–alkyne 1,3-dipolar cycloaddition (Haldón *et al.*, 2015), a cornerstone of click chemistry, which enables the facile synthesis of 1,4-regioisomeric 1,2,3-triazoles. A wide variety of synthetic routes to 1,2,3-triazoles and their derivatives, employing various metal catalysts, organocatalysts, as well as catalyst- and solvent-free reactions, have been developed in the past two decades (Vala *et al.*, 2022).

1,2,3-Triazole-containing hybrids have attracted our interest because of their potential as antitubercular agents (Tan *et al.*,

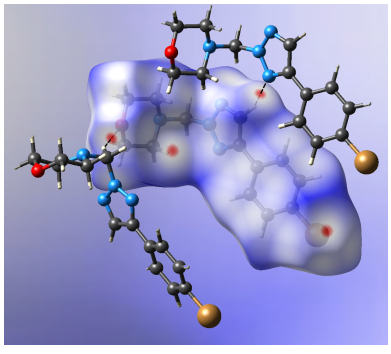

Table 1
Experimental details.

For both structures: $Z = 4$. Experiments were carried out at 100 K with Mo $K\alpha$ radiation. The absorption correction was Gaussian (*SADABS*; Bruker, 2016). All H-atom parameters were refined.

	3	**4a**
Crystal data		
Chemical formula	$C_{17}H_{11}BrN_4O_2$	$C_{13}H_{15}BrN_4O$
M_r	383.21	323.19
Crystal system, space group	Monoclinic, $P2_1/n$	Monoclinic, $P2_1/c$
a, b, c (Å)	8.9293 (5), 5.4537 (3), 31.0109 (16)	16.5886 (11), 5.7516 (4), 14.3116 (11)
β (°)	93.347 (2)	104.348 (2)
V (Å^3)	1507.58 (14)	1322.89 (16)
μ (mm^{-1})	2.75	3.11
Crystal size (mm)	0.52 × 0.07 × 0.04	0.08 × 0.02 × 0.02
Data collection		
Diffractometer	Bruker Kappa Mach3 APEXII	Bruker D8 Venture
T_{min}, T_{max}	0.607, 0.906	0.872, 0.960
No. of measured, independent and observed [$I \geq 2\sigma(I)$] reflections	56275, 5290, 4650	197950, 3296, 2614
R_{int}	0.037	0.158
$(\sin\theta/\lambda)_{max}$ (Å^{-1})	0.750	0.668
Refinement		
$R[F^2 > 2\sigma(F^2)]$, $wR(F^2)$, S	0.018, 0.029, 1.06	0.026, 0.057, 1.07
No. of reflections	5290	3296
No. of parameters	286	257
$\Delta\rho_{max}$, $\Delta\rho_{min}$ (e Å^{-3})	0.31, −0.29	0.58, −0.49

Computer programs: *APEX5* (Bruker, 2022), *SAINT* (Bruker, 2019), *SHELXT* (Sheldrick, 2015*b*), *olex2.refine* (Bourhis *et al.*, 2015), *DIAMOND* (Brandenburg, 2018) and *publCIF* (Westrip, 2010).

2021; Scarim & Pavan, 2021). Herein, we report on the synthesis and structural characterization of an example in which the heterocycle links an *N*-phthalimidylmethyl and a 4-(4-bromophenyl) group. Post-click functionalization of the molecule (Yadav *et al.*, 2025) with morpholine (Tzara *et al.*, 2020) resulted in a formal migration of the methylene bridge from N1 to N2 on the triazole ring, while replacing the phthalimide group in a nucleophilic substitution reaction, as proven by X-ray crystallography.

2. Experimental

2.1. General

Starting materials and reagents were purchased and used as received. Solvents were distilled before use. The synthesis of *N*-(azidomethyl)phthalimide from *N*-(bromomethyl)phthalimide can be found in the literature (Zhang *et al.*, 2013). The NMR spectrum of **3** in chloroform-*d* was recorded on a Varian INOVA 500 spectrometer and those of **3** and **4a**/**4b** (see supporting information) in acetonitrile-d_3 on a Bruker Avance Neo 600 spectrometer (abbreviations: *s* = singlet, *dd* = doublet of doublets and *m* = multiplet). Chemical shifts are reported relative to the residual solvent signals.

2.2. Synthesis and crystallization

2.2.1. 2-[4-(4-Bromophenyl)-1*H*-1,2,3-triazol-1-yl)methyl]-isoindoline-1,3-dione (3)

N-(Azidomethyl)phthalimide (607 mg, 3.00 mmol) and 1-bromo-4-ethynylbenzene (543 mg, 3.00 mmol) were suspended in *tert*-butyl alcohol/water (50 ml, 1:1 *v*/*v*) with ultrasonication. $CuSO_4{\cdot}5H_2O$ (7.5 mg, 0.03 mmol) and 0.3 ml of a 1 *M* aqueous solution of sodium ascorbate (0.3 mmol) were added, and the mixture was stirred vigorously overnight until it became clear. Subsequently, water (50 ml) was added and the solution was extracted thrice with ethyl acetate (30 ml). The combined organic layers were dried over anhydrous sodium sulfate. The crude product was purified by flash chromatography (silica gel, dichloromethane/methanol gradient) to yield **3** (746 mg, 1.95 mmol, 65%) as a white solid. ^{1}H NMR (502 MHz, chloroform-*d*): δ 8.10 (*s*, 1H), 7.93 (*dd*, J = 5.5, 3.1 Hz, 2H), 7.79 (*dd*, J = 5.5, 3.1 Hz, 2H), 7.73–7.67 (*m*, 2H), 7.56–7.50 (*m*, 2H), 6.25 (*s*, 2H). ^{13}C{^{1}H} NMR (126 MHz, chloroform-*d*): δ 166.7, 147.6, 135.1, 132.1, 131.6, 129.3, 127.5, 124.4, 122.5, 120.7, 50.0. ^{1}H NMR (600.20 MHz, acetonitrile-d_3): 8.29 (*s*, 1H), 7.91 (*m*, 2H), 7.84 (*m*, 2H), 7.78 (*m*, 2H), 7.59 (*m*, 2H), 6.16 (*s*, 2H). ^{13}C{^{1}H} NMR (150.94 MHz, acetonitrile-d_3): δ 167.0, 147.4, 135.9, 132.9, 132.7, 130.9, 128.4, 124.6, 122.7, 122.4, 51.2. A crystal of **3** suitable for single-crystal X-ray diffraction analysis was obtained from a solution in chloroform-*d* after the solvent had been evaporated slowly at room temperature.

2.2.2. 4-{[4-(4-Bromophenyl)-2*H*-1,2,3-triazol-2-yl]methyl}-morpholine (4a) and 4-{[4-(4-bromophenyl)-1*H*-1,2,3-triazol-1-yl)methyl]morpholine (4b)

Compound **3** (300 mg, 0.78 mmol) was dissolved in acetonitrile (5 ml) and triethylamine (506 mg, 5.00 mmol) and morpholine (96 mg, 1.10 mmol) were added with stirring. The reaction mixture was heated to 85 °C for 12 h. After cooling to room temperature, water (30 ml) was added. The colourless

precipitate so obtained was filtered off and dried in the air. A crystal of **4a** suitable for single-crystal X-ray diffraction analysis was obtained from a solution in acetonitrile after the solvent had evaporated slowly under ambient conditions.

2.3. X-ray crystallography

After initial independent atom model (IAM) refinements with *SHEXL2019* (Sheldrick, 2015*a*), the crystal structures of **3** and **4a** were refined with aspherical atomic form factors using *NoSpherA2* (Kleemiss *et al.*, 2021; Midgley *et al.*, 2021) in *OLEX2* (Dolomanov *et al.*, 2009). Hirshfeld-partitioned electron density was calculated in *ORCA* (Version 5.0; Neese *et al.*, 2020) using the B3LYP hybrid functional (Becke, 1993; Lee *et al.*, 1988) and the def2-TZVPP basis set (Weigend & Ahlrichs, 2005). Anisotropic atomic displacement parameters (ADPs) were introduced for all non-H atoms. Positions and isotropic ADPs were refined freely for all H atoms. The ADPs of the Br atom in both **3** and **4a** were refined anharmonically to fourth order using the Gram–Charlier series in *OLEX2*. Although the resolution of the diffraction data does not strictly obey Kuhs' rule (Kuhs, 1988), according to which an estimated resolution of $(\sin\theta/\lambda)_{max} = 1.01$ Å^{-1} (*cf* Table 1) is required to resolve anharmonic atomic displacements, refinement of the Gram–Charlier parameters resulted in flat difference electron-density maps near the Br atoms (Herbst-Irmer *et al.*, 2013) and in a drop in $wR(F^2)$ from 0.0368 to 0.0294 for **3** and from 0.0625 to 0.0571 for **4a**. F_o–F_c(HAR) difference electron-density maps with and without anharmonically refined ADPs for Br atoms, as well as the corresponding Henn–Meindl fractal dimension plots (Meindl & Henn, 2008), are shown in Fig. S1 in the supporting information. F_c(HAR)–F_c(IAM) deformation density maps and the corresponding F_o–F_c(IAM) difference maps are shown in Fig. S2.

Packing indices were calculated with *PLATON* (Spek, 2020). Hirshfeld surface analysis was conducted with *CrystalExplorer* (Spackman *et al.*, 2021), which normalizes *X*—H bond lengths to standard neutron-derived values (Allen & Bruno, 2010). Crystal data, data collection and structure refinement details are listed in Table 1.

2.4. Computational methods

Density functional theory (DFT) calculations on the free molecules of **4a** and **4b** were performed using *ORCA* (Version 6.0; Neese, 2025) with a B3LYP/G (VWN1) hybrid functional (20% HF exchange) and a def2-TZVPP basis set (Weigend & Ahlrichs, 2005) with an auxiliary def2/J basis (Weigend, 2006). The starting geometry for **4a** was taken from the crystal structure, and that for **4b** was built using *Avogadro* (Hanwell *et al.*, 2012). Optimization of the structures used the BFGS method from an initial Hessian according to Almlöf's model with a very tight self-consistent field convergence threshold (Fletcher, 2000). The optimized local minimum-energy structures exhibited only positive modes. A conformational search was performed using the Global Optimization Algorithm (GOAT; de Souza, 2025) and an extended semi-empirical tight-binding model (Bannwarth *et al.*, 2019). The six lowest energy conformations so obtained were subsequently optimized as described above and indicate that the conformations described are global minima on the potential energy surface. Cartesian coordinates of the DFT-optimized structures of **4a** and **4b** can be found in the supporting information.

3. Results and discussion

3.1. Chemistry

The chemistry employed in this work is outlined in Fig. 1. The 1,2,3-triazole **3** was synthesized from *N*-(azidomethyl) phthalimide (**1**) and the terminal alkyne 1-bromo-4-ethynylbenzene (**2**) using the traditional click-chemistry method, employing a copper-catalyzed 1,3-dipolar cycloaddition reaction (Haldón *et al.*, 2015). After flash chromatography, compound **3** was obtained in satisfactory yield. ^{1}H and ^{13}C NMR spectroscopy in acetonitrile-d_3 confirmed the structure of the anticipated 1,4-regioisomeric 1,2,3-triazole with no signs of isomerization to the N^2-substituted form (Katritzky *et al.*,

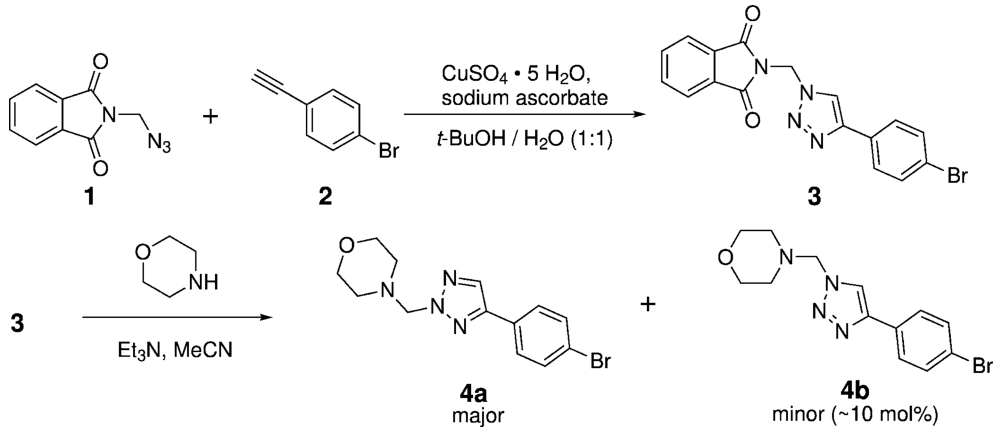

Figure 1
Two-step synthesis of **4a** starting from *N*-(azidomethyl)phthalimide (**1**) and 1-bromo-4-ethynylbenzene (**2**). The amount of the minor component **4b** was estimated from NMR analysis in acetonitrile-d_3 (see supporting information).

Table 2
Hydrogen-bond geometry (Å, °) for **3**.

D—H···A	D—H	H···A	D···A	D—H···A
C5—H5···N2^{i}	1.051 (9)	2.431 (9)	3.4527 (9)	163.8 (7)
C5—H5···N3^{i}	1.051 (9)	2.356 (9)	3.3625 (9)	160.0 (7)
C13—H13···O3^{ii}	1.058 (9)	2.259 (9)	3.2941 (9)	165.5 (7)
C16—H16···O1^{iii}	1.075 (9)	2.370 (9)	3.4281 (9)	167.9 (7)

Symmetry codes: (i) $x, y-1, z$; (ii) $-x+2, -y+1, -z+2$; (iii) $-x+1, -y+3, -z+2$.

2010). X-ray crystallography established the molecular structure of **3** in the solid state.

In the second step, compound **3** was reacted with morpholine in acetonitrile in the presence of triethylamine as a base. Crystal structure analysis revealed that morpholine replaced the phthalimide group on the methylene group in a nucleophilic substitution reaction, accompanied by a migration of the methylene bridge from N1 to N2 on the 1,2,3-triazole ring to form the N^2-substituted isomer **4a** as the major component. Telegina *et al.* (2016) previously described a similar migration of an N^1-(ferrocenylmethyl) group upon alkylation of a 1,2,3-triazole. In the present work, NMR analysis in acetonitrile-d_3 showed that the N^1-substituted isomer **4b** was present as a minor component (see supporting information), which could not be separated and crystallographically characterized in the present work. It is known that *N*-(α-aminoalkyl)-1,2,3-triazoles can isomerize between their N^1- and N^2-substituted isomers in solution. The equilibrium depends on the electron-withdrawing effect of the groups bonded to the amino N atom and the polarity of the solvent (Katritzky *et al.*, 2010).

According to DFT calculations on the free molecules, isomer **4a** is more stable than **4b** by 5 kcal mol^{-1}. This energy difference is similar to that reported for N^1- and N^2-(ferrocenylmethyl)-substituted 1,2,3-triazoles (Telegina *et al.*, 2016). For the parent 1,2,3-triazole, the 2*H*-tautomer was reported to be about 4.5 kcal mol^{-1} more stable than the 1*H*-tautomer in the gas phase (Katritzky *et al.*, 2010).

3.2. Crystal and molecular structure of 3

Fig. 2 depicts the molecular structure of **3** in the crystal. The triazole ring and the benzene ring are significantly twisted about the C3—C4 bond, with an angle between the respective mean planes of 23.12 (4)°. The phthalimide moiety is virtually planar and the angle between its mean plane and that of the triazole ring linked by the methylene bridge is 69.45 (3)°, resulting in an angular structure of the molecule, as also encountered in the crystal structure of the related N^1-(1*H*-1,2,3-benzotriazol-1-ylmethyl)phthalimide (CSD refcode HOFPEY; Wang *et al.*, 2008).

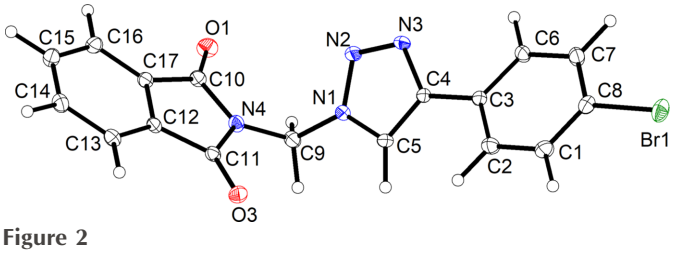

Figure 2
The molecular structure of **3** in the crystal. Displacement ellipsoids are drawn at the 50% probability level. H atoms are shown as small spheres of arbitrary radius.

In the crystal, the molecules are densely packed with a Kitajgorodskij packing index (Kitajgorodskij, 1973) of 73.1%. Although close packing seems to dominate the solid-state structure, some intermolecular contacts shorter than the sum of the corresponding van der Waals radii (Bondi, 1964) are indicative of weak hydrogen bonds (Table 2). The triazole C—H group forms a donating weak bifurcated C—H···N hydrogen bond to the N atoms of the triazole moiety of a neighbouring molecule related by translational symmetry in the crystallographic *b*-axis direction. The phthalimide groups of adjacent molecules are each joined *via* two weak C—H···O hydrogen bonds between the C—H groups in the 4- and 7-positions, and the carbonyl O atoms with a centrosymmetric $R_2^2(10)$ motif (Bernstein *et al.*, 1995), resulting in tapes along the [$\bar{1}$20] direction (Fig. 3). Halogen bonding is absent in the crystal structure of **3**.

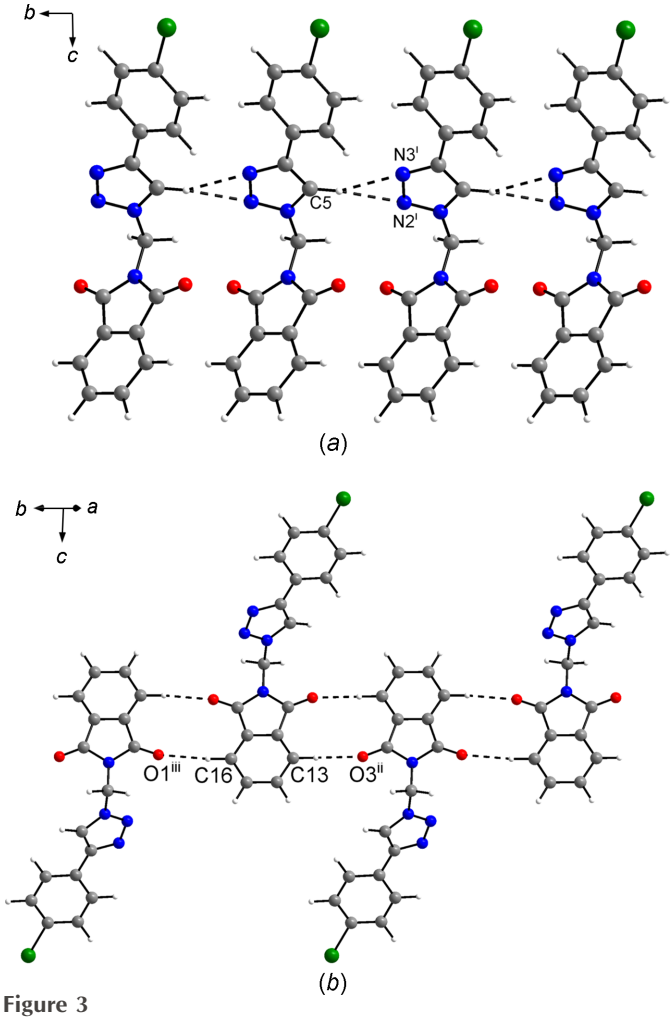

Figure 3
Sections of the crystal structure of **3**, viewed (*a*) along the *a*-axis direction and (*b*) along the [110] direction. Dashed lines represent weak hydrogen bonds. Colour scheme: C grey, H white, Br green, N blue and O red. [Symmetry codes: (i) $x, y-1, z$; (ii) $-x+2, -y+1, -z+2$; (iii) $-x+1, -y+3, -z+2$.]

Table 3
Hydrogen-bond geometry (Å, °) for **4a**.

D—H···A	D—H	H···A	D···A	D—H···A
C5—H5···N3^{i}	1.06 (3)	2.57 (3)	3.572 (3)	158.3 (19)
C9—H9A···O1^{ii}	1.11 (2)	2.47 (2)	3.481 (2)	150.3 (15)
C9—H9B···N1^{iii}	1.10 (2)	2.66 (2)	3.696 (3)	157.7 (17)
C11—H11A···O1^{iv}	1.08 (2)	2.67 (2)	3.426 (3)	126.2 (16)
C12—H12A···O1^{v}	1.07 (2)	2.62 (2)	3.661 (2)	166.0 (16)
C13—H13A···N4^{vi}	1.08 (2)	2.63 (2)	3.553 (2)	142.4 (16)

Symmetry codes: (i) $x, y+1, z$; (ii) $x, -y+\frac{1}{2}, z-\frac{1}{2}$; (iii) $x, y-1, z$; (iv) $-x, -y, -z+1$; (v) $-x, -y+1, -z+1$; (vi) $-x, y+\frac{1}{2}, -z+\frac{1}{2}$.

3.3. Crystal and molecular structure of 4a

Fig. 4 shows the molecular structure of **4a** in the crystal. The tilt angle between the mean planes through the triazole ring and the benzene ring is slightly less than in **3** at 18.3 (1)°. As expected, the morpholine six-membered aliphatic heterocycle adopts a low-energy chair conformation, with the *N*-methylene group in the equatorial position, resulting in an angular shape of the molecule.

A Kitajgorodskij packing index (Kitajgorodskij, 1973) of 73.1% was calculated for **4a**, likewise indicating a dense crystal packing. The central motif in the crystal packing is a centrosymmetric dimeric arrangement of the molecules (Fig. 5). The separation between the mean planes through the benzene rings in the molecules constituting a dimer is 3.55 Å and the corresponding centroid–centroid distance is 3.724 (1) Å, which is typical of face-to-face aromatic stacking. Within a dimer, the morpholine O atom approaches the Br atom of the symmetry-related molecule, but the O···Br distance (longer than the sum of the corresponding van der Waals radii at 3.71 Å; Bondi, 1964) and the O···Br—C angle (150.2°) are not indicative of halogen bonding. The crystal structure features several C—H···N and C—H···O short contacts that can be regarded as weak intermolecular hydrogen bonds (Table 3). Worth noting are those formed between the triazole C—H group and an N atom of the triazole ring of an adjacent molecule (C5—H5···N3^{i}) and those formed between the two methylene C—H groups and the morpholine O atom (C9—H9A···O1^{ii}) and a triazole N atom (C9—H9B···N1^{iii}) of neighbouring molecules (Fig. 6).

A search of the Cambridge Structural Database (CSD; Groom *et al.*, 2016) revealed only a few examples of structurally characterized 2-aminomethyl-1,2,3-triazoles related to

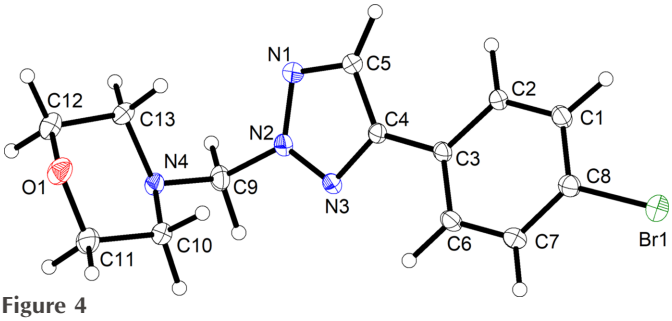

Figure 4
The molecular structure of **4a** in the crystal. Displacement ellipsoids are drawn at the 50% probability level. H atoms are shown as small spheres of arbitrary radius.

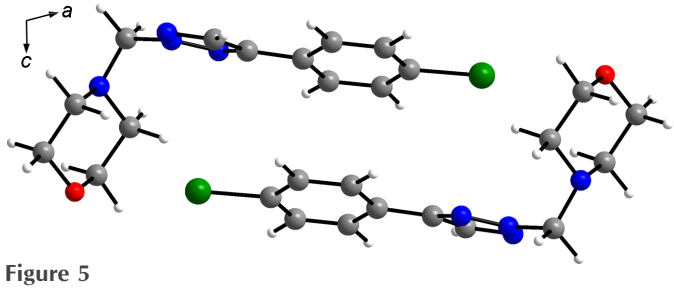

Figure 5
Centrosymmetric dimeric arrangement of the molecules in the crystal structure of **4a**, viewed along the *b*-axis direction. Colour scheme: C grey, H white, Br green, N blue and O red.

4a. For example, 1-(4-bromophenyl)-*N*-methyl-*N*-[(4-phenyl-2*H*-1,2,3-triazol-2-yl)methyl]methanamine (CSD refcode ZETXII; Gupta *et al.*, 2018) and *N*,*N*-dibenzyl-1-[4-(4-fluorophenyl)-2*H*-1,2,3-triazol-2-yl]methanamine (AKITEV; Jiang *et al.*, 2016). Like in **4a**, the N—N—C—N torsion angle in these structures is close to 90 °C.

3.4. Hirshfeld surface analysis

In order to gain insight into the molecular environments of **3** and **4a** in the crystal structures, we performed Hirshfeld surface analyses (Spackman & Jayatilaka, 2009). Figs. 7(*a*) and 7(*b*) show the Hirshfeld surfaces for **3** and **4a** mapped with the normalized contact distance (d_{norm}), whereby the colours

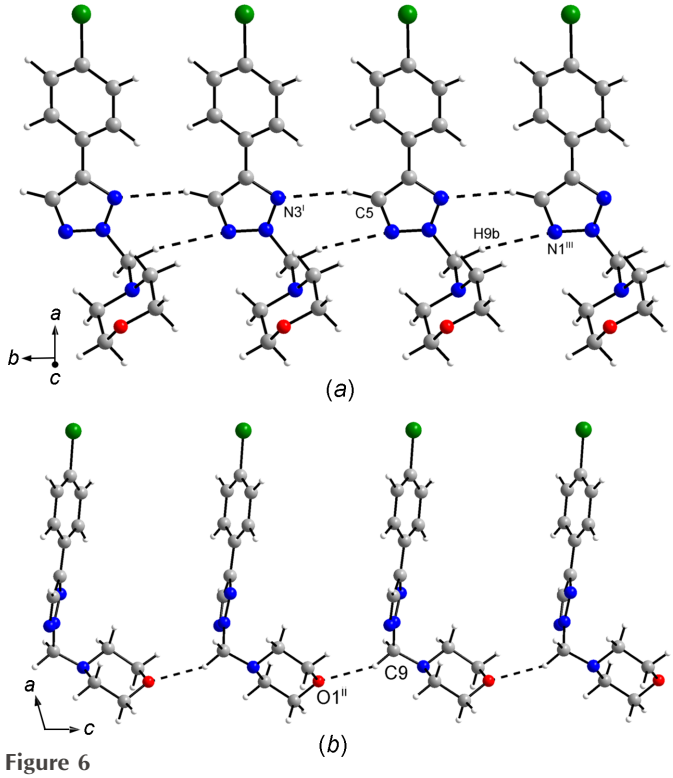

Figure 6
Sections of the crystal structure of **4a**, viewed (*a*) approximately along the *c*-axis direction and (*b*) along the *b*-axis direction. Dashed lines represent weak hydrogen bonds. Colour scheme: C grey, H white, Br green, N blue and O red. [Symmetry codes: (i) $x, y+1, z$; (ii) $x, -y+\frac{1}{2}, z-\frac{1}{2}$; (iii) $x+1, y-1, z$.]

indicate intermolecular contacts shorter (red), approximately equal (white) or longer (blue) than the sum of the van der Waals radii. The pronounced red-coloured concave areas on the Hirshfeld surface for **3** [Fig. 7(*a*)] correspond to the weak C—H···O and bifurcated C—H···N hydrogen bonds described in Section 3.2. Inspection of the d_{norm} plot for **4a** reveals that the C—H···O and C—H···N interactions are less significant than in **3**; the respective red areas on the Hirshfeld surface are smaller [Fig. 7(*b*)].

As expected, the corresponding 2D fingerprint plot for **3** shows characteristic spikes of the O···H/H···O contacts resulting from the weak C—H···O hydrogen bonds. The N···H/H···N contacts from the weak bifurcated C—H···N hydrogen bonds give rise to more diffuse wing-like features. In contrast, the fingerprint plot for **4a** is more diffuse as a whole than that for **3**, indicating that H···H contacts from close packing are more frequent (44.6% of the surface area) than in **3** (21.9%). Whereas small spikes from Br···H/H···Br contacts are present for both structures, C···H/H···C contacts resulting from edge-to-face (C—H···π) aromatic stacking are observed only for **4a**. A triangular feature on the centre of the diagonal characteristic of face-to-face aromatic stacking is not pronounced either in **3** and **4a**.

4. Conclusions

In this article, we have reported the synthesis of the 1,2,3-triazole **3** bearing an N^1-phthalimidylmethyl group through click chemistry and its structural characterization by X-ray crystallography. The crystal structure of **3** features weak intermolecular hydrogen bonds of the C—H···O type between the phthalimidyl groups and of the C—H···N type

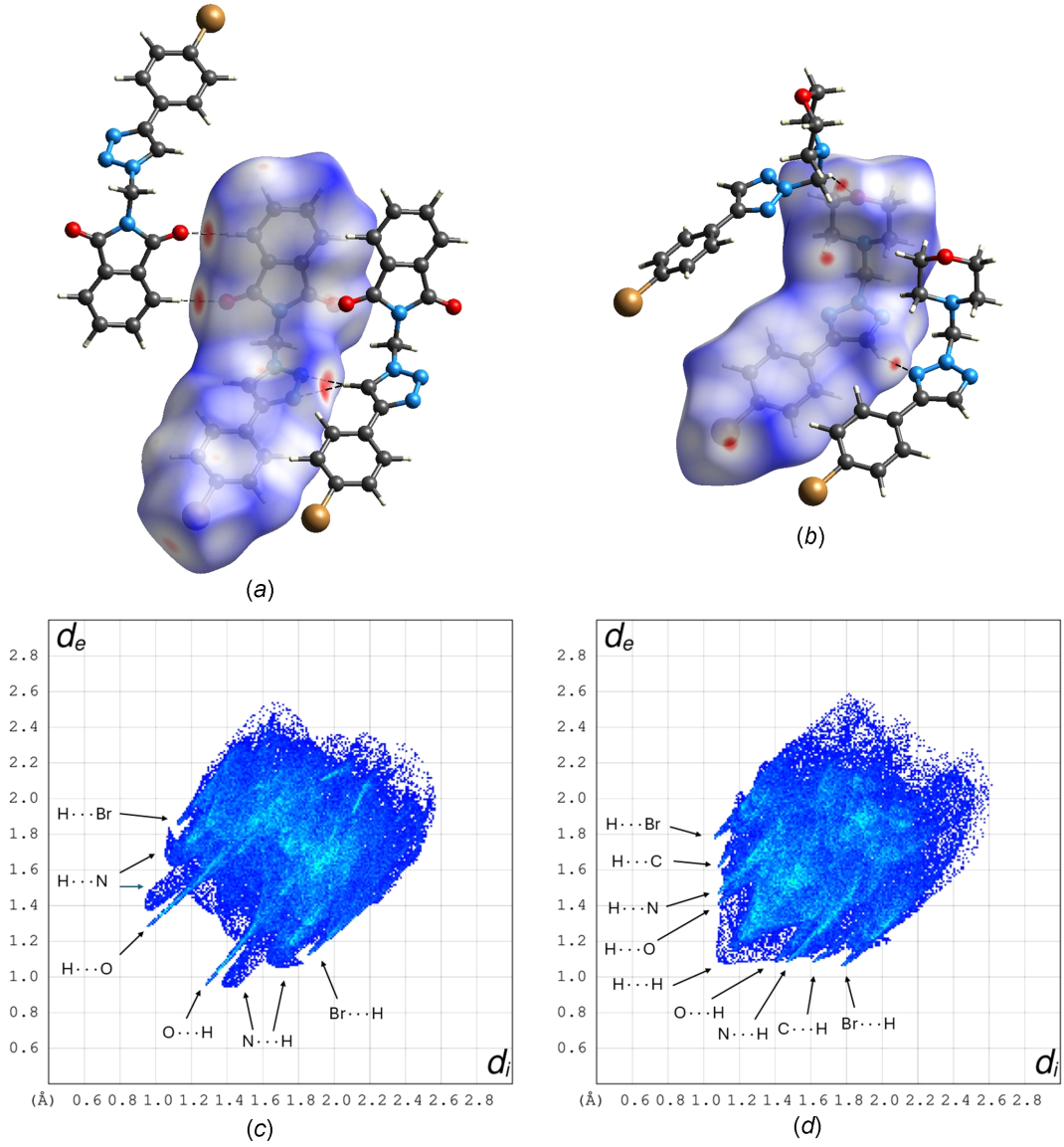

Figure 7
Hirshfeld surface mapped with d_{norm} for (*a*) **3** and (*b*) **4a**, and the corresponding fingerprint plots (*c*) and (*d*). d_i is the distance from a point on the Hirshfeld surface to the nearest nucleus inside the surface (*i.e.* belonging to the reference molecule) and d_e is the distance from the same surface point to the nearest nucleus outside the surface (*i.e.* in any neighbouring molecule). Dashed lines show weak hydrogen bonds. Colour scheme for the atoms: C grey, H white, Br bronze, N blue and O red.

between the triazole rings of adjacent molecules. X-ray crystallography provided clear evidence that the bridging methylene group underwent a migration from N1 to N2 on the triazole ring in the major product **4a**, resulting from a nucleophilic substitution of the phthalimidyl group in **3** with morpholine. DFT calculations on the free molecules indicate that **4a** is lower in energy than the N^1-substituted structural isomer **4b**, which was detected as a minor product. Examples of similar migrations of nitrogen-bound substituents on 1,2,3-triazoles appear to be scarce.

Acknowledgements

We would like to thank Professor Christian W. Lehmann for providing access to the X-ray diffraction facility and Heike Salandin for technical assistance with the X-ray intensity data collections. Open access funding enabled and organized by Projekt DEAL.

Funding information

Funding for this research was provided by: German Research Foundation (DFG) (grant No. 432291016 to Adrian Richter).

References

Allen, F. H. & Bruno, I. J. (2010). *Acta Cryst.* B**66**, 380–386.
Bannwarth, C., Ehlert, S. & Grimme, S. (2019). *J. Chem. Theory Comput.* **15**, 1652–1671.
Becke, A. D. (1993). *J. Chem. Phys.* **98**, 5648–5652.
Bernstein, J., Davis, R. E., Shimoni, L. & Chang, N.-L. (1995). *Angew. Chem. Int. Ed. Engl.* **34**, 1555–1573.
Bonandi, E., Christodoulou, M. S., Fumagalli, G., Perdicchia, D., Rastelli, G. & Passarella, D. (2017). *Drug Discov. Today* **22**, 1572–1581.
Bondi, A. (1964). *J. Phys. Chem.* **68**, 441–451.
Bourhis, L. J., Dolomanov, O. V., Gildea, R. J., Howard, J. A. K. & Puschmann, H. (2015). *Acta Cryst.* A**71**, 59–75.
Bozorov, K., Zhao, J. & Aisa, H. A. (2019). *Bioorg. Med. Chem.* **27**, 3511–3531.
Brandenburg, K. (2018). *DIAMOND*. Version 3.2k4. Crystal Impact GbR, Bonn, Germany.
Bruker (2016). *SADABS*. Bruker AXS Inc., Madison, Wisconsin, USA.
Bruker (2019). *SAINT*. Bruker AXS Inc., Madison, Wisconsin, USA.
Bruker (2022). *APEX5*. Bruker AXS Inc., Madison, Wisconsin, USA.
Dai, J., Tian, S., Yang, X. & Liu, Z. (2022). *Front. Chem.* **10**, 891484.
de Souza, B. (2025). *Angew. Chem. Int. Ed.* **64**, e202500393.
Dolomanov, O. V., Bourhis, L. J., Gildea, R. J., Howard, J. A. K. & Puschmann, H. (2009). *J. Appl. Cryst.* **42**, 339–341.
Farwa, U., Arif, M., Farhan, M., Sandhu, Z. A., Oirdi, M. E., Aatif, M., Nahvi, I. & Raza, M. A. (2025). *Arab. J. Chem.* **18**, 802025.
Fletcher, R. (2000). In *Practical Methods of Optimization*, 2nd ed. New York: John Wiley & Sons.
Groom, C. R., Bruno, I. J., Lightfoot, M. P. & Ward, S. C. (2016). *Acta Cryst.* B**72**, 171–179.
Gupta, S., Chandna, N., Singh, A. K. & Jain, N. (2018). *J. Org. Chem.* **83**, 3226–3235.
Haldón, E., Nicasio, M. C. & Pérez, P. J. (2015). *Org. Biomol. Chem.* **13**, 9528–9550.
Hanwell, M. D., Curtis, D. E., Lonie, D. C., Vandermeersch, T., Zurek, E. & Hutchison, G. R. (2012). *J. Cheminform* **4**, 17.
Herbst-Irmer, R., Henn, J., Holstein, J. J., Hübschle, C. B., Dittrich, B., Stern, D., Kratzert, D. & Stalke, D. (2013). *J. Phys. Chem. A* **117**, 633–641.
Jiang, Y., Wang, Q., Sun, R., Tang, X.-Y. & Shi, M. (2016). *Org. Chem. Front.* **3**, 744–748.
Katritzky, A. R., Buciumas, A., Todadze, E., Ali Munawar, M. & Khelashvili, L. (2010). *Heterocycles* **82**, 479.
Kitajgorodskij, A. I. (1973). In *Molecular crystals and molecules*. London: Academic Press.
Kleemiss, F., Dolomanov, O. V., Bodensteiner, M., Peyerimhoff, N., Midgley, M., Bourhis, L. J., Genoni, A., Malaspina, L. A., Jayatilaka, D., Spencer, J. L., White, F., Grundkötter-Stock, B., Steinhauer, S., Lentz, D., Puschmann, H. & Grabowsky, S. (2021). *Chem. Sci.* **12**, 1675–1692.
Kuhs, W. F. (1988). *Aust. J. Phys.* **41**, 369–382.
Lee, C., Yang, W. & Parr, R. G. (1988). *Phys. Rev. B* **37**, 785–789.
Marzi, M., Farjam, M., Kazeminejad, Z., Shiroudi, A., Kouhpayeh, A. & Zarenezhad, E. (2022). *J. Chem.* **2022**, 7884316.
Meindl, K. & Henn, J. (2008). *Acta Cryst.* A**64**, 404–418.
Midgley, L., Bourhis, L. J., Dolomanov, O. V., Grabowsky, S., Kleemiss, F., Puschmann, H. & Peyerimhoff, N. (2021). *Acta Cryst.* A**77**, 519–533.
Moura, N. M. M. & Tomé, A. C. (2022). *1,2,3-Triazoles*, in *Comprehensive Heterocyclic Chemistry IV*, edited by D. StC Black, J. Cossy & C. V. Stevens, pp. 1–77. Amsterdam: Elsevier.
Neese, F. (2025). *WIREs Comput. Mol. Sci.* **15**, e70019.
Neese, F., Wennmohs, F., Becker, U. & Riplinger, C. (2020). *J. Chem. Phys.* **152**, 224108.
Scarim, C. B. & Pavan, F. R. (2021). *Eur. J. Med. Chem. Rep.* **1**, 100002.
Sheldrick, G. M. (2015*a*). *Acta Cryst.* C**71**, 3–8.
Sheldrick, G. M. (2015*b*). *Acta Cryst.* A**71**, 3–8.
Song, H., Wang, S., Cai, Q. & Chen, J. (2024). *J. Heterocycl. Chem.* **61**, 365–386.
Spackman, M. A. & Jayatilaka, D. (2009). *CrystEngComm* **11**, 19–32.
Spackman, P. R., Turner, M. J., McKinnon, J. J., Wolff, S. K., Grimwood, D. J., Jayatilaka, D. & Spackman, M. A. (2021). *J. Appl. Cryst.* **54**, 1006–1011.
Spek, A. L. (2020). *Acta Cryst.* E**76**, 1–11.
Tan, Z., Deng, J., Ye, Q. & Zhang, Z. (2021). *Future Med. Chem.* **13**, 643–662.
Telegina, L. N., Kelbysheva, E. S., Strelkova, T. V., Ezernitskaya, M. G., Borisov, Y. A., Smol'yakov, A. F., Peregudov, A. S., Rodionov, A. N., Ikonnikov, N. S. & Loim, N. M. (2016). *Eur. J. Org. Chem.* **2016**, 5897–5906.
Tzara, A., Xanthopoulos, D. & Kourounakis, A. P. (2020). *ChemMedChem* **15**, 392–403.
Vala, D. P., Vala, R. M. & Patel, H. M. (2022). *ACS Omega* **7**, 36945–36987.
Verma, C., Goni, L. K. M. O., Yaagoob, I. Y., Alyami, R. A., Alfantazi, A. & Mazumder, M. A. J. (2026). *J. Organomet. Chem.* **1043**, 123900.
Wang, S.-Q., Jian, F.-F. & Liu, H.-Q. (2008). *Acta Cryst.* E**64**, o1782.
Weigend, F. (2006). *Phys. Chem. Chem. Phys.* **8**, 1057–1065.
Weigend, F. & Ahlrichs, R. (2005). *Phys. Chem. Chem. Phys.* **7**, 3297–3305.
Westrip, S. P. (2010). *J. Appl. Cryst.* **43**, 920–925.
Yadav, M. S., Pandey, V. K., Jaiswal, M. K., Singh, S. K., Sharma, A., Singh, M. & Tiwari, V. K. (2025). *J. Org. Chem.* **90**, 5731–5762.
Zhang, S., Zhang, W.-X. & Xi, Z. (2013). *Angew. Chem. Int. Ed.* **52**, 3485–3489.

supporting information

Acta Cryst. (2026). C**82**, 144-150 [https://doi.org/10.1107/S2053229626002810]

Nucleophilic substitution of a phthalimidyl group with morpholine in an N^1-methyl-1,2,3-triazole: crystallographic evidence for migration of the methylene bridge

Paul R. Palme, Richard Goddard, Markus Leutzsch, Adrian Richter, Peter Imming and Rüdiger W. Seidel

Computing details

2-{[4-(4-Bromophenyl)-1*H*-1,2,3-triazol-1-yl]methyl}isoindoline-1,3-dione (3)

Crystal data

$C_{17}H_{11}BrN_4O_2$
M_r = 383.21
Monoclinic, $P2_1/n$
a = 8.9293 (5) Å
b = 5.4537 (3) Å
c = 31.0109 (16) Å
β = 93.347 (2)°
V = 1507.58 (14) Å^3
Z = 4
$F(000)$ = 767.675
D_x = 1.688 Mg m^{-3}
Mo $K\alpha$ radiation, λ = 0.71073 Å
Cell parameters from 9905 reflections
θ = 2.3–31.9°
μ = 2.75 mm^{-1}
T = 100 K
Needle, colourless
0.52 × 0.07 × 0.04 mm

Data collection

Bruker Kappa Mach3 APEXII diffractometer
Radiation source: microfocus X-ray tube
Incoatec Helios mirrors monochromator
Detector resolution: 66.67 pixels mm^{-1}
φ and ω–scans
Absorption correction: gaussian (SADABS; Bruker, 2016)
T_{min} = 0.607, T_{max} = 0.906
56275 measured reflections
5290 independent reflections
4650 reflections with $I \geq 2\sigma(I)$
R_{int} = 0.037
θ_{max} = 32.2°, θ_{min} = 1.3°
h = −13→13
k = −8→8
l = −46→46

Refinement

Refinement on F^2
Least-squares matrix: full
$R[F^2 > 2\sigma(F^2)]$ = 0.018
$wR(F^2)$ = 0.029
S = 1.06
5290 reflections
286 parameters
0 restraints
0 constraints
Primary atom site location: dual
Secondary atom site location: difference Fourier map
Hydrogen site location: difference Fourier map
All H-atom parameters refined
$w = 1/[\sigma^2(F_o^2) + (0.0027P)^2 + 0.1953P]$ where $P = (F_o^2 + 2F_c^2)/3$
$(\Delta/\sigma)_{max}$ = 0.0001
$\Delta\rho_{max}$ = 0.31 e Å^{-3}
$\Delta\rho_{min}$ = −0.29 e Å^{-3}

Special details

Experimental. Crystal mounted on a MiTeGen loop using Perfluoropolyether PFO-XR75

Refinement. Refinement using NoSpherA2, an implementation of NOn-SPHERical Atom-form-factors in Olex2. Please cite: F. Kleemiss *et al.* Chem. Sci. DOI 10.1039/D0SC05526C - 2021 NoSpherA2 implementation of HAR makes use of tailor-made aspherical atomic form factors calculated on-the-fly from a Hirshfeld-partitioned electron density (ED) - not from spherical-atom form factors.
The ED is calculated from a gaussian basis set single determinant SCF wavefunction - either Hartree-Fock or DFT using selected funtionals - for a fragment of the crystal. This fragment can be embedded in an electrostatic crystal field by employing cluster charges or modelled using implicit solvation models, depending on the software used. The following options were used: SOFTWARE: ORCA 5.0 PARTITIONING: NoSpherA2 INT ACCURACY: Normal METHOD: B3LYP BASIS SET: def2-TZVPP CHARGE: 0 MULTIPLICITY: 1 DATE: 2025-10-10_10-10-56
The minimum and maximum estimated transmissions from the multi-scan scaling are 0.6170 and 0.9142 (SADABS).

Fractional atomic coordinates and isotropic or equivalent isotropic displacement parameters (Å²)

	x	*y*	*z*	U_{iso}*/U_{eq}
C1	1.09578 (8)	0.62059 (14)	0.74243 (2)	0.01829 (15)
H1	1.1590 (11)	0.4528 (18)	0.7407 (3)	0.039 (3)*
C2	1.01239 (9)	0.67052 (13)	0.77791 (2)	0.01761 (15)
H2	1.0095 (10)	0.5397 (17)	0.8033 (3)	0.035 (2)*
C3	0.93169 (8)	0.88896 (12)	0.78024 (2)	0.01279 (13)
C4	0.84024 (8)	0.93920 (12)	0.81690 (2)	0.01239 (13)
C5	0.77681 (8)	0.77863 (13)	0.84497 (2)	0.01387 (13)
H5	0.7788 (10)	0.5865 (17)	0.8476 (3)	0.030 (2)*
C6	0.93634 (8)	1.05796 (13)	0.74651 (2)	0.01516 (14)
H6	0.8727 (10)	1.2252 (16)	0.7483 (3)	0.030 (2)*
C7	1.01968 (8)	1.01040 (14)	0.71093 (2)	0.01685 (14)
H7	1.0241 (10)	1.1456 (17)	0.6849 (3)	0.030 (2)*
C8	1.09750 (8)	0.79109 (14)	0.70924 (2)	0.01633 (14)
C9	0.60496 (8)	0.85200 (14)	0.90571 (2)	0.01519 (14)
H9a	0.5913 (10)	0.6560 (17)	0.9041 (3)	0.033 (2)*
H9b	0.4987 (10)	0.9473 (16)	0.9014 (3)	0.031 (2)*
C10	0.63000 (8)	1.12561 (13)	0.97094 (2)	0.01355 (13)
C11	0.77981 (8)	0.77588 (12)	0.97000 (2)	0.01278 (13)
C12	0.81228 (7)	0.90437 (12)	1.01170 (2)	0.01205 (13)
C13	0.91075 (8)	0.84212 (13)	1.04605 (2)	0.01486 (14)
H13	0.9778 (10)	0.6823 (16)	1.0454 (3)	0.027 (2)*
C14	0.91697 (8)	0.99981 (14)	1.08162 (2)	0.01704 (14)
H14	0.9927 (10)	0.9572 (16)	1.1085 (3)	0.034 (2)*
C15	0.82819 (9)	1.21079 (14)	1.08217 (2)	0.01834 (15)
H15	0.8371 (10)	1.3273 (17)	1.1100 (3)	0.037 (2)*
C16	0.72940 (8)	1.27219 (13)	1.04718 (2)	0.01595 (14)
H16	0.6593 (10)	1.4323 (16)	1.0472 (3)	0.028 (2)*
C17	0.72359 (7)	1.11411 (12)	1.01213 (2)	0.01288 (13)
Br1	1.208372 (19)	0.71938 (3)	0.660554 (5)	0.02242 (7)
N1	0.69881 (7)	0.92386 (10)	0.870981 (18)	0.01323 (12)
N2	0.71288 (7)	1.16131 (11)	0.86040 (2)	0.01588 (12)
N3	0.79877 (7)	1.17127 (11)	0.827776 (19)	0.01513 (12)
N4	0.67053 (7)	0.91830 (11)	0.947420 (18)	0.01384 (12)

O1	0.53505 (6)	1.27154 (9)	0.958973 (17)	0.01931 (11)
O3	0.83162 (6)	0.58929 (9)	0.956210 (16)	0.01723 (11)

Atomic displacement parameters (Å²)

	U^{11}	U^{22}	U^{33}	U^{12}	U^{13}	U^{23}
C1	0.0203 (4)	0.0147 (3)	0.0201 (4)	0.0028 (3)	0.0033 (3)	−0.0014 (3)
C2	0.0220 (4)	0.0134 (3)	0.0177 (4)	0.0031 (3)	0.0033 (3)	0.0017 (3)
C3	0.0160 (3)	0.0112 (3)	0.0111 (3)	0.0006 (2)	0.0000 (3)	−0.0001 (2)
C4	0.0163 (3)	0.0102 (3)	0.0105 (3)	0.0003 (2)	0.0000 (3)	0.0000 (2)
C5	0.0183 (3)	0.0094 (3)	0.0138 (3)	−0.0003 (3)	0.0002 (3)	0.0006 (2)
C6	0.0188 (3)	0.0143 (3)	0.0124 (3)	0.0033 (3)	0.0010 (3)	0.0018 (3)
C7	0.0196 (4)	0.0180 (4)	0.0130 (3)	0.0024 (3)	0.0014 (3)	0.0014 (3)
C8	0.0160 (3)	0.0176 (3)	0.0155 (3)	−0.0005 (3)	0.0018 (3)	−0.0034 (3)
C9	0.0157 (3)	0.0153 (3)	0.0145 (3)	−0.0014 (3)	0.0006 (3)	0.0021 (3)
C10	0.0129 (3)	0.0135 (3)	0.0143 (3)	0.0022 (3)	0.0018 (3)	0.0014 (3)
C11	0.0140 (3)	0.0115 (3)	0.0130 (3)	0.0023 (2)	0.0029 (2)	0.0020 (2)
C12	0.0126 (3)	0.0122 (3)	0.0116 (3)	0.0014 (2)	0.0026 (2)	0.0023 (2)
C13	0.0140 (3)	0.0158 (3)	0.0148 (3)	0.0012 (3)	0.0012 (3)	0.0032 (3)
C14	0.0170 (3)	0.0203 (4)	0.0138 (3)	−0.0022 (3)	0.0000 (3)	0.0018 (3)
C15	0.0214 (4)	0.0183 (3)	0.0155 (3)	−0.0025 (3)	0.0028 (3)	−0.0020 (3)
C16	0.0183 (3)	0.0137 (3)	0.0162 (3)	0.0007 (3)	0.0041 (3)	−0.0012 (3)
C17	0.0134 (3)	0.0123 (3)	0.0131 (3)	0.0012 (2)	0.0025 (3)	0.0009 (2)
Br1	0.02140 (12)	0.02850 (12)	0.01792 (11)	−0.00173 (8)	0.00603 (8)	−0.00716 (8)
N1	0.0165 (3)	0.0117 (3)	0.0115 (3)	−0.0005 (2)	0.0005 (2)	0.0010 (2)
N2	0.0221 (3)	0.0105 (3)	0.0154 (3)	0.0020 (2)	0.0044 (2)	0.0001 (2)
N3	0.0215 (3)	0.0093 (3)	0.0149 (3)	0.0009 (2)	0.0038 (2)	0.0017 (2)
N4	0.0152 (3)	0.0141 (3)	0.0123 (3)	0.0026 (2)	0.0011 (2)	0.0013 (2)
O1	0.0179 (3)	0.0170 (3)	0.0228 (3)	0.0066 (2)	−0.0009 (2)	0.0013 (2)
O3	0.0199 (3)	0.0134 (2)	0.0185 (3)	0.0048 (2)	0.0019 (2)	−0.0008 (2)

Geometric parameters (Å, º)

C1—H1	1.078 (10)	C9—N4	1.4345 (9)
C1—C2	1.3912 (10)	C10—C17	1.4864 (10)
C1—C8	1.3877 (10)	C10—N4	1.4042 (9)
C2—H2	1.063 (9)	C10—O1	1.2055 (8)
C2—C3	1.3963 (10)	C11—C12	1.4845 (10)
C3—C4	1.4640 (9)	C11—N4	1.4021 (9)
C3—C6	1.3965 (9)	C11—O3	1.2064 (8)
C4—C5	1.3794 (9)	C12—C13	1.3834 (10)
C4—N3	1.3664 (9)	C12—C17	1.3917 (9)
C5—H5	1.051 (9)	C13—H13	1.058 (9)
C5—N1	1.3523 (9)	C13—C14	1.3973 (10)
C6—H6	1.078 (9)	C14—H14	1.067 (9)
C6—C7	1.3909 (10)	C14—C15	1.3980 (11)
C7—H7	1.096 (9)	C15—H15	1.070 (9)
C7—C8	1.3858 (10)	C15—C16	1.3984 (11)

C8—Br1	1.8940 (7)	C16—H16	1.075 (9)
C9—H9a	1.076 (9)	C16—C17	1.3860 (10)
C9—H9b	1.083 (9)	N1—N2	1.3435 (8)
C9—N1	1.4565 (9)	N2—N3	1.3059 (8)
C2—C1—H1	120.7 (5)	O1—C10—C17	129.97 (7)
C8—C1—H1	120.3 (5)	O1—C10—N4	124.73 (7)
C8—C1—C2	119.02 (7)	N4—C11—C12	105.56 (6)
H2—C2—C1	119.4 (5)	O3—C11—C12	130.35 (7)
C3—C2—C1	120.63 (7)	O3—C11—N4	124.09 (7)
C3—C2—H2	120.0 (5)	C13—C12—C11	129.64 (6)
C4—C3—C2	120.84 (6)	C17—C12—C11	108.31 (6)
C6—C3—C2	119.10 (6)	C17—C12—C13	122.06 (7)
C6—C3—C4	120.04 (6)	H13—C13—C12	121.5 (5)
C5—C4—C3	129.75 (6)	C14—C13—C12	116.81 (7)
N3—C4—C3	122.44 (6)	C14—C13—H13	121.7 (5)
N3—C4—C5	107.77 (6)	H14—C14—C13	118.4 (5)
H5—C5—C4	132.5 (5)	C15—C14—C13	121.32 (7)
N1—C5—C4	104.43 (6)	C15—C14—H14	120.2 (5)
N1—C5—H5	123.0 (5)	H15—C15—C14	118.9 (5)
H6—C6—C3	118.7 (5)	C16—C15—C14	121.34 (7)
C7—C6—C3	120.78 (7)	C16—C15—H15	119.8 (5)
C7—C6—H6	120.5 (5)	H16—C16—C15	122.4 (5)
H7—C7—C6	120.2 (5)	C17—C16—C15	116.91 (7)
C8—C7—C6	118.92 (7)	C17—C16—H16	120.7 (5)
C8—C7—H7	120.9 (5)	C12—C17—C10	108.55 (6)
C7—C8—C1	121.54 (7)	C16—C17—C10	129.88 (6)
Br1—C8—C1	118.80 (5)	C16—C17—C12	121.57 (7)
Br1—C8—C7	119.66 (6)	C9—N1—C5	128.47 (6)
H9b—C9—H9a	112.0 (7)	N2—N1—C5	111.11 (6)
N1—C9—H9a	107.6 (5)	N2—N1—C9	120.39 (6)
N1—C9—H9b	108.6 (5)	N3—N2—N1	107.26 (5)
N4—C9—H9a	109.3 (5)	N2—N3—C4	109.42 (5)
N4—C9—H9b	107.3 (5)	C10—N4—C9	124.55 (6)
N4—C9—N1	112.13 (6)	C11—N4—C9	123.10 (6)
N4—C10—C17	105.27 (6)	C11—N4—C10	112.31 (6)
C1—C2—C3—C4	178.19 (7)	C9—N4—C10—C17	178.38 (7)
C1—C2—C3—C6	−0.35 (9)	C9—N4—C10—O1	0.35 (8)
C1—C8—C7—C6	−0.97 (9)	C9—N4—C11—C12	−178.04 (7)
C2—C3—C4—C5	−23.63 (9)	C9—N4—C11—O3	2.03 (7)
C2—C3—C4—N3	158.91 (7)	C10—C17—C12—C11	0.65 (6)
C2—C3—C6—C7	0.15 (8)	C10—C17—C12—C13	−179.33 (5)
C3—C4—C5—N1	−177.05 (8)	C10—C17—C16—C15	178.97 (7)
C3—C4—N3—N2	177.31 (7)	C10—N4—C11—C12	−0.14 (6)
C3—C6—C7—C8	0.50 (8)	C10—N4—C11—O3	179.93 (5)
C4—C5—N1—C9	177.56 (5)	C11—C12—C13—C14	−179.70 (7)
C4—C5—N1—N2	−0.54 (7)	C11—C12—C17—C16	179.97 (5)

C4—N3—N2—N1	0.30 (6)	C12—C13—C14—C15	−0.33 (8)
C5—N1—C9—N4	110.48 (8)	C12—C17—C16—C15	−0.20 (8)
C5—N1—N2—N3	0.16 (6)	C13—C14—C15—C16	0.14 (8)
C6—C7—C8—Br1	178.70 (6)	C14—C15—C16—C17	0.13 (8)
C9—N1—N2—N3	−178.11 (7)		

Hydrogen-bond geometry (Å, º)

D—H···*A*	*D*—H	H···*A*	*D*···*A*	*D*—H···*A*
C5—H5···N2^{i}	1.051 (9)	2.431 (9)	3.4527 (9)	163.8 (7)
C5—H5···N3^{i}	1.051 (9)	2.356 (9)	3.3625 (9)	160.0 (7)
C13—H13···O3^{ii}	1.058 (9)	2.259 (9)	3.2941 (9)	165.5 (7)
C16—H16···O1^{iii}	1.075 (9)	2.370 (9)	3.4281 (9)	167.9 (7)

Symmetry codes: (i) *x*, *y*−1, *z*; (ii) −*x*+2, −*y*+1, −*z*+2; (iii) −*x*+1, −*y*+3, −*z*+2.

4-{[4-(4-Bromophenyl)-2*H*-1,2,3-triazol-2-yl]methyl}morpholine (4a)

Crystal data

$C_{13}H_{15}BrN_4O$
M_r = 323.19
Monoclinic, $P2_1/c$
a = 16.5886 (11) Å
b = 5.7516 (4) Å
c = 14.3116 (11) Å
β = 104.348 (2)°
V = 1322.89 (16) Å^3
Z = 4
$F(000)$ = 655.573
D_x = 1.623 Mg m^{-3}
Mo $K\alpha$ radiation, λ = 0.71073 Å
Cell parameters from 9522 reflections
θ = 2.5–21.8°
μ = 3.11 mm^{-1}
T = 100 K
Needle, colourless
0.08 × 0.02 × 0.02 mm

Data collection

Bruker D8 Venture diffractometer
Radiation source: microfocus X-ray tube
Montel multilayer optics monochromator
Detector resolution: 7.391 pixels mm^{-1}
φ and ω–scans
Absorption correction: gaussian (SADABS; Bruker, 2016)
T_{min} = 0.872, T_{max} = 0.960
197950 measured reflections
3296 independent reflections
2614 reflections with $I \geq 2\sigma(I)$
R_{int} = 0.158
θ_{max} = 28.3°, θ_{min} = 2.5°
h = −22→22
k = −7→7
l = −19→18

Refinement

Refinement on F^2
Least-squares matrix: full
$R[F^2 > 2\sigma(F^2)]$ = 0.026
$wR(F^2)$ = 0.057
S = 1.07
3296 reflections
257 parameters
0 restraints
0 constraints
Primary atom site location: dual
Secondary atom site location: difference Fourier map
Hydrogen site location: difference Fourier map
All H-atom parameters refined
$w = 1/[\sigma^2(F_o^2) + (0.0173P)^2 + 0.8578P]$ where $P = (F_o^2 + 2F_c^2)/3$
$(\Delta/\sigma)_{max}$ = −0.0002
$\Delta\rho_{max}$ = 0.58 e Å^{-3}
$\Delta\rho_{min}$ = −0.49 e Å^{-3}

Special details

Experimental. Crystal mounted on a MiTeGen loop using Perfluoropolyether Fomblin YR-1800

Refinement. Refinement using NoSpherA2, an implementation of NOn-SPHERical Atom-form-factors in Olex2. Please cite: F. Kleemiss *et al.* Chem. Sci. DOI 10.1039/D0SC05526C - 2021 NoSpherA2 implementation of HAR makes use of tailor-made aspherical atomic form factors calculated on-the-fly from a Hirshfeld-partitioned electron density (ED) - not from spherical-atom form factors.
The ED is calculated from a gaussian basis set single determinant SCF wavefunction - either Hartree-Fock or DFT using selected funtionals - for a fragment of the crystal. This fragment can be embedded in an electrostatic crystal field by employing cluster charges or modelled using implicit solvation models, depending on the software used. The following options were used: SOFTWARE: ORCA 5.0 PARTITIONING: NoSpherA2 INT ACCURACY: Normal METHOD: B3LYP BASIS SET: def2-TZVPP CHARGE: 0 MULTIPLICITY: 1 DATE: 2024-07-21_19-25-06
Estimated minimum and maximum transmission: 0.8500 0.9643 The ratio of these values is more reliable than their absolute values!

Fractional atomic coordinates and isotropic or equivalent isotropic displacement parameters (Å²)

	x	*y*	*z*	U_{iso}*/U_{eq}
C1	0.57106 (12)	0.6433 (3)	0.36447 (13)	0.0182 (4)
H1	0.6079 (14)	0.784 (4)	0.3499 (16)	0.035 (6)*
C2	0.48515 (11)	0.6411 (3)	0.33054 (13)	0.0167 (4)
H2	0.4521 (14)	0.789 (4)	0.2893 (17)	0.038 (6)*
C3	0.43877 (11)	0.4494 (3)	0.34785 (12)	0.0148 (3)
C4	0.34852 (11)	0.4485 (3)	0.30857 (13)	0.0160 (4)
C5	0.29518 (12)	0.6349 (4)	0.27320 (15)	0.0212 (4)
H5	0.3101 (15)	0.813 (5)	0.2701 (18)	0.046 (7)*
C6	0.48057 (12)	0.2611 (3)	0.40014 (14)	0.0186 (4)
H6	0.4454 (13)	0.115 (4)	0.4121 (15)	0.028 (5)*
C7	0.56686 (12)	0.2619 (3)	0.43380 (14)	0.0192 (4)
H7	0.5968 (14)	0.123 (4)	0.4746 (17)	0.040 (6)*
C8	0.61105 (11)	0.4536 (3)	0.41488 (13)	0.0175 (4)
C9	0.15261 (12)	0.1691 (4)	0.23232 (14)	0.0188 (4)
H9a	0.1114 (13)	0.242 (4)	0.1658 (15)	0.025 (5)*
H9b	0.1765 (15)	0.000 (4)	0.2161 (17)	0.035 (6)*
C10	0.15991 (12)	0.0363 (4)	0.39511 (14)	0.0186 (4)
H10a	0.2151 (15)	0.144 (4)	0.4304 (16)	0.036 (6)*
H10b	0.1809 (15)	−0.135 (4)	0.3741 (17)	0.041 (6)*
C11	0.10695 (13)	0.0025 (3)	0.46715 (16)	0.0233 (4)
H11a	0.0573 (15)	−0.119 (4)	0.4380 (17)	0.040 (6)*
H11b	0.1434 (16)	−0.064 (4)	0.5357 (18)	0.044 (7)*
C12	0.02071 (13)	0.3115 (4)	0.40202 (15)	0.0226 (4)
H12a	−0.0053 (14)	0.466 (4)	0.4234 (16)	0.031 (5)*
H12b	−0.0303 (14)	0.193 (4)	0.3707 (16)	0.037 (6)*
C13	0.07135 (12)	0.3612 (3)	0.32940 (15)	0.0196 (4)
H13a	0.0311 (14)	0.424 (4)	0.2626 (16)	0.031 (6)*
H13b	0.1198 (15)	0.488 (4)	0.3611 (17)	0.038 (6)*
N1	0.21828 (10)	0.5539 (3)	0.24013 (12)	0.0218 (4)
N2	0.22590 (10)	0.3260 (3)	0.25533 (11)	0.0179 (3)
N3	0.30240 (10)	0.2535 (3)	0.29613 (11)	0.0169 (3)
N4	0.10975 (9)	0.1459 (3)	0.30736 (11)	0.0169 (3)

O1	0.07189 (9)	0.2164 (2)	0.48814 (10)	0.0240 (3)
Br1	0.72856 (3)	0.45850 (8)	0.45815 (3)	0.0213 (2)

Atomic displacement parameters (Å²)

	U^{11}	U^{22}	U^{33}	U^{12}	U^{13}	U^{23}
C1	0.0200 (10)	0.0162 (9)	0.0208 (9)	−0.0028 (8)	0.0094 (8)	0.0000 (8)
C2	0.0174 (9)	0.0144 (9)	0.0210 (9)	0.0002 (7)	0.0099 (7)	0.0020 (7)
C3	0.0177 (9)	0.0130 (8)	0.0165 (8)	−0.0009 (7)	0.0094 (7)	−0.0003 (7)
C4	0.0169 (9)	0.0133 (8)	0.0207 (9)	−0.0004 (7)	0.0103 (7)	−0.0009 (8)
C5	0.0181 (9)	0.0147 (9)	0.0338 (11)	0.0014 (8)	0.0124 (8)	0.0034 (8)
C6	0.0226 (10)	0.0143 (9)	0.0216 (10)	−0.0015 (8)	0.0106 (8)	0.0024 (7)
C7	0.0211 (10)	0.0161 (9)	0.0211 (10)	0.0005 (8)	0.0067 (8)	0.0040 (8)
C8	0.0211 (9)	0.0166 (9)	0.0165 (8)	−0.0002 (8)	0.0077 (7)	0.0000 (8)
C9	0.0174 (9)	0.0215 (11)	0.0196 (10)	−0.0021 (8)	0.0088 (8)	−0.0011 (8)
C10	0.0178 (9)	0.0174 (9)	0.0226 (9)	0.0015 (8)	0.0086 (7)	0.0011 (8)
C11	0.0251 (10)	0.0249 (12)	0.0236 (10)	0.0036 (8)	0.0128 (8)	0.0030 (8)
C12	0.0191 (10)	0.0260 (11)	0.0244 (10)	0.0034 (8)	0.0088 (8)	−0.0027 (8)
C13	0.0178 (9)	0.0183 (9)	0.0241 (10)	0.0047 (8)	0.0078 (8)	0.0009 (8)
N1	0.0187 (8)	0.0155 (8)	0.0331 (9)	0.0018 (7)	0.0104 (7)	0.0047 (7)
N2	0.0171 (8)	0.0166 (8)	0.0227 (8)	−0.0010 (6)	0.0102 (6)	0.0005 (6)
N3	0.0174 (7)	0.0134 (8)	0.0226 (8)	−0.0016 (6)	0.0098 (6)	0.0006 (6)
N4	0.0158 (8)	0.0165 (8)	0.0203 (8)	0.0001 (6)	0.0083 (6)	−0.0019 (6)
O1	0.0250 (7)	0.0272 (8)	0.0224 (7)	0.0046 (6)	0.0109 (6)	−0.0015 (6)
Br1	0.0180 (3)	0.0250 (3)	0.0214 (3)	0.0008 (2)	0.0058 (2)	−0.0009 (2)

Geometric parameters (Å, º)

C1—H1	1.07 (2)	C9—N2	1.484 (2)
C1—C2	1.387 (3)	C9—N4	1.434 (2)
C1—C8	1.383 (3)	C10—H10a	1.12 (2)
C2—H2	1.10 (2)	C10—H10b	1.11 (3)
C2—C3	1.401 (3)	C10—C11	1.524 (3)
C3—C4	1.463 (2)	C10—N4	1.466 (2)
C3—C6	1.399 (3)	C11—H11a	1.08 (2)
C4—C5	1.403 (3)	C11—H11b	1.09 (3)
C4—N3	1.344 (2)	C11—O1	1.424 (2)
C5—H5	1.06 (3)	C12—H12a	1.07 (2)
C5—N1	1.330 (3)	C12—H12b	1.09 (2)
C6—H6	1.06 (2)	C12—C13	1.517 (3)
C6—C7	1.393 (3)	C12—O1	1.421 (2)
C7—H7	1.04 (2)	C13—H13a	1.08 (2)
C7—C8	1.387 (3)	C13—H13b	1.10 (2)
C8—Br1	1.8937 (19)	C13—N4	1.463 (2)
C9—H9a	1.11 (2)	N1—N2	1.329 (2)
C9—H9b	1.10 (2)	N2—N3	1.326 (2)
C2—C1—H1	121.9 (12)	C11—C10—H10b	110.0 (13)

C8—C1—H1	118.5 (12)	N4—C10—H10a	112.2 (12)
C8—C1—C2	119.58 (18)	N4—C10—H10b	107.4 (12)
H2—C2—C1	120.8 (12)	N4—C10—C11	109.54 (15)
C3—C2—C1	120.44 (18)	H11a—C11—C10	109.5 (13)
C3—C2—H2	118.8 (12)	H11b—C11—C10	111.8 (13)
C4—C3—C2	119.28 (17)	H11b—C11—H11a	108.7 (18)
C6—C3—C2	118.86 (17)	O1—C11—C10	111.51 (16)
C6—C3—C4	121.83 (17)	O1—C11—H11a	109.2 (12)
C5—C4—C3	129.05 (18)	O1—C11—H11b	106.1 (13)
N3—C4—C3	123.26 (17)	H12b—C12—H12a	108.0 (17)
N3—C4—C5	107.62 (16)	C13—C12—H12a	111.8 (12)
H5—C5—C4	128.6 (13)	C13—C12—H12b	110.0 (12)
N1—C5—C4	108.90 (18)	O1—C12—H12a	105.6 (12)
N1—C5—H5	122.5 (13)	O1—C12—H12b	110.6 (12)
H6—C6—C3	118.7 (12)	O1—C12—C13	110.71 (16)
C7—C6—C3	120.90 (17)	H13a—C13—C12	110.1 (12)
C7—C6—H6	120.4 (12)	H13b—C13—C12	108.4 (13)
H7—C7—C6	119.9 (13)	H13b—C13—H13a	111.7 (17)
C8—C7—C6	118.85 (18)	N4—C13—C12	109.43 (16)
C8—C7—H7	121.2 (13)	N4—C13—H13a	107.4 (11)
C7—C8—C1	121.36 (18)	N4—C13—H13b	109.9 (12)
Br1—C8—C1	118.71 (14)	N2—N1—C5	104.09 (16)
Br1—C8—C7	119.93 (15)	N1—N2—C9	121.58 (15)
H9b—C9—H9a	109.5 (16)	N3—N2—C9	123.26 (15)
N2—C9—H9a	104.9 (11)	N3—N2—N1	115.09 (15)
N2—C9—H9b	105.5 (12)	N2—N3—C4	104.30 (15)
N4—C9—H9a	111.3 (11)	C10—N4—C9	113.59 (15)
N4—C9—H9b	110.3 (12)	C13—N4—C9	113.95 (15)
N4—C9—N2	114.94 (15)	C13—N4—C10	111.38 (15)
H10b—C10—H10a	109.6 (17)	C12—O1—C11	109.68 (15)
C11—C10—H10a	108.1 (12)		

C1—C2—C3—C4	−178.05 (17)	C4—N3—N2—C9	−177.05 (13)
C1—C2—C3—C6	0.2 (2)	C4—N3—N2—N1	−0.07 (17)
C1—C8—C7—C6	0.7 (2)	C5—N1—N2—C9	177.15 (14)
C2—C3—C4—C5	−16.7 (2)	C5—N1—N2—N3	0.11 (18)
C2—C3—C4—N3	159.72 (16)	C6—C7—C8—Br1	−179.17 (14)
C2—C3—C6—C7	−0.7 (2)	C9—N4—C10—C11	−175.63 (17)
C3—C4—C5—N1	176.9 (2)	C9—N4—C13—C12	174.31 (17)
C3—C4—N3—N2	−177.08 (18)	C10—C11—O1—C12	59.95 (19)
C3—C6—C7—C8	0.2 (2)	C10—N4—C13—C12	−55.59 (16)
C4—C5—N1—N2	−0.10 (18)	C11—O1—C12—C13	−61.14 (16)

Hydrogen-bond geometry (Å, º)

D—H···*A*	*D*—H	H···*A*	*D*···*A*	*D*—H···*A*
C5—H5···N3^{i}	1.06 (3)	2.57 (3)	3.572 (3)	158.3 (19)
C9—H9*a*···O1^{ii}	1.11 (2)	2.47 (2)	3.481 (2)	150.3 (15)

C9—H9*b*···N1^{iii}	1.10 (2)	2.66 (2)	3.696 (3)	157.7 (17)
C11—H11*a*···O1^{iv}	1.08 (2)	2.67 (2)	3.426 (3)	126.2 (16)
C12—H12*a*···O1^{v}	1.07 (2)	2.62 (2)	3.661 (2)	166.0 (16)
C13—H13*a*···N4^{vi}	1.08 (2)	2.63 (2)	3.553 (2)	142.4 (16)

Symmetry codes: (i) *x*, *y*+1, *z*; (ii) *x*, −*y*+1/2, *z*−1/2; (iii) *x*, *y*−1, *z*; (iv) −*x*, −*y*, −*z*+1; (v) −*x*, −*y*+1, −*z*+1; (vi) −*x*, *y*+1/2, −*z*+1/2.